

## CMS results on B-Physics

---

**Bora Akgün\***

*Rice University*

*E-mail:* [bora.akgun@cern.ch](mailto:bora.akgun@cern.ch)

The observation of a new  $b$  baryon via its strong decay into  $\Xi_b^- \pi^+$  (plus charge conjugates) is reported. The measurement uses a data sample of  $pp$  collisions at  $\sqrt{s} = 7$  TeV collected by the CMS experiment at the LHC, corresponding to an integrated luminosity of  $5.3 \text{ fb}^{-1}$ . The new state most likely corresponds to the  $J^P = 3/2^+$  companion of the  $\Xi_b$ .

A flavour-untagged measurement of the lifetime difference in the  $B_s \rightarrow J/\psi \phi$  with  $J/\psi \rightarrow \mu^+ \mu^-$  and  $\phi \rightarrow K^+ K^-$  decay is presented. Assuming the mixing phase  $\phi_s$  to be zero, we obtain a decay width difference  $\Delta\Gamma_s = 0.048 \pm 0.024$  (stat.)  $\pm 0.003$  (syst.)  $ps^{-1}$  between the two  $B_s$  mass eigenstates.

The  $\Lambda_b$  differential production cross section and the cross-section ratio  $\sigma(\bar{\Lambda}_b)/\sigma(\Lambda_b)$  are measured as functions of transverse momentum  $p_T^{\Lambda_b}$  and rapidity  $|y^{\Lambda_b}|$  in  $pp$  collisions at  $\sqrt{s} = 7$  TeV. The measurements are based on  $\Lambda_b$  decays reconstructed in the exclusive final state  $J/\psi \Lambda$ , with the subsequent decays  $J/\psi \rightarrow \mu^+ \mu^-$  and  $\Lambda \rightarrow p\pi$ , using a data sample corresponding to an integrated luminosity of  $1.9 \text{ fb}^{-1}$ .

*LHC on the March - IHEP-LHC,*

*20-22 November 2012*

*Institute for High Energy Physics, Protvino, Moscow region, Russia*

---

\*Speaker.

## 1. Observation of a new $\Xi_b$ baryon

This section presents a search for the decay  $\Xi_b^{*0} \rightarrow \Xi_b^- \pi^+$ , with  $\Xi_b^- \rightarrow J/\psi \Xi^-$ ,  $J/\psi \rightarrow \mu^+ \mu^-$ ,  $\Xi^- \rightarrow \Lambda^0 \pi^-$ , and  $\Lambda^0 \rightarrow p \pi^-$ . Charge conjugate states are implied throughout. The reconstruction of such decays involves the presence of three secondary vertices, where the  $\Xi_b^-$ ,  $\Xi^-$ , and  $\Lambda^0$  decay, which are well separated from the primary interaction vertex. We measure the difference ( $Q$ ) between the  $\Xi_b^{*0}$  mass and the sum of the masses of its decay products  $Q = M_{inv}(J/\psi \Xi^- \pi^+) - M_{inv}(J/\psi \Xi^-) - m_\pi$ , where  $M_{inv}$  stands for invariant mass and  $m_\pi$  is the world average charged pion mass [1].

The reconstruction of the  $\Xi_b^- \rightarrow J/\psi \Xi^-$  candidates begins by identifying  $J/\psi \rightarrow \mu^+ \mu^-$  decays. Candidate  $J/\psi$  mesons are reconstructed by combining pairs of oppositely charged muons having an invariant mass within 150 MeV of the nominal  $J/\psi$  mass [1]. Candidate  $\Lambda^0$  baryons are reconstructed in decays to a pion ( $\pi_\Lambda$ ) and a proton with opposite charge where the higher momentum track is assumed to be the proton. Possible contamination from mis-reconstructed  $K_s$  mesons is removed by requiring the candidate mass, when assuming both tracks are pions, to be out of a 20 MeV window around the  $K_s$  nominal mass [1]. Candidate  $\Xi^-$  baryons are reconstructed by combining a  $\Lambda^0$  candidate with a track ( $\pi_\Xi$ ) of the same charge sign as the  $\pi_\Lambda$ . A veto of a 20 MeV window around the  $\Omega$  nominal mass [1] is applied when assuming that the  $\pi_\Xi$  is a kaon. The  $\Xi^-$  candidate is then combined with the  $J/\psi$  candidate to form a  $\Xi_b^-$  candidate with a kinematic vertex fit, constraining their masses to the world average values. The primary vertex (PV) where the  $\Xi_b^-$  has been created is chosen by taking the closest vertex to the  $\Xi_b^-$  trajectory.

The  $\Xi_b^-$  signal selection cuts have been chosen by an iterative algorithm, which looks for the maximum  $S/\sqrt{S+B}$  within the  $\Xi_b^-$  mass peak, while never allowing the  $\Xi_b^-$  signal yield to decrease. As displayed in Fig. 1(left) the measured mass is  $5795.0 \pm 3.1(\text{stat.})$  MeV which is in good agreement with [1] and the measured resolution is  $23.7 \pm 3.2(\text{stat.})$  MeV with a signal yield of  $108 \pm 14$  events.

To reconstruct candidate  $\Xi_b^{*0}$  baryons, the  $\Xi_b^-$  candidates, with a mass within  $2.5\sigma$  of the signal peak, are combined with tracks, assumed to be pions, whose trajectory distance to the chosen PV is  $< 3\sigma$  and whose charge is opposite to the pion from the  $\Xi^-$  decay (right sign). We search for narrow resonances in the  $Q$  mass difference distribution. To model the background shape of the  $Q$  variable, the events in which the pions from the  $\Xi_b^{*0}$  and the  $\Xi_b^-$  decays have the same sign (wrong sign candidates) are used.

The measured opposite-sign  $Q$  distribution is displayed in Fig. 1(right) for the range 0-50 MeV. The 21 events observed in the region  $12 < Q < 18$  MeV represent a clear excess with respect to the expected background yield of  $3.0 \pm 1.4$  events, evaluated by integrating the background function in this  $Q$  window. An un-binned maximum-likelihood fit is performed to the opposite-sign  $Q$  distribution with a Breit-Wigner distribution convolved with a Gaussian function, added to the background function previously described. The fitted parameters of the peak are  $Q = 14.84 \pm 0.74$  (stat.) MeV and Breit-Wigner width  $\Gamma = 2.1 \pm 1.7$  (stat.) MeV. The systematic uncertainty on the measured  $Q$  value is evaluated through a detailed MC simulation and found to be 0.26 MeV.

In summary, a new neutral  $\Xi_b$  baryon has been discovered with  $5.0 fb^{-1}$  of CMS data with a significance of  $6.6\sigma$ . The measured  $Q = M_{inv}(J/\psi \Xi^- \pi^+) - M_{inv}(J/\psi \Xi^-) - m_\pi$  value is  $14.81 \pm 0.74(\text{stat.}) \pm 0.26(\text{syst.})$  MeV. According to theory predictions the new baryon is the  $\Xi_b^{*0}$ , with

$J = 3/2$ .

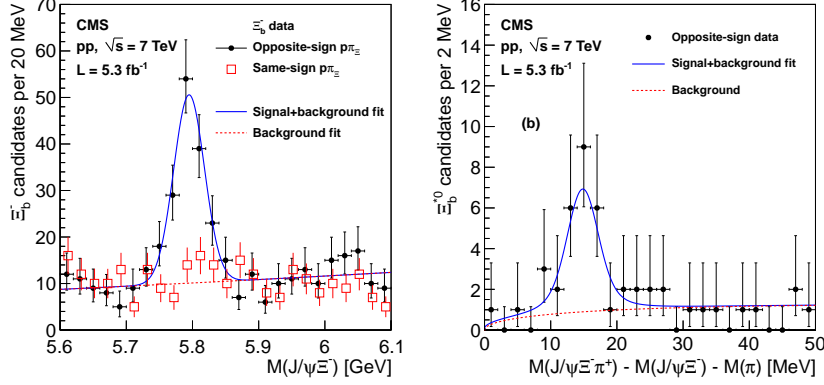


**Figure 1:** (Left) Invariant-mass distributions of the selected  $B_s^-$  candidates (closed circles) and of the  $J/\psi\pi\pi^-$  pairs where the proton and  $\pi^-$  have the same charge (open squares). The blue solid curve represents the result of the signal-plus-background fit to the  $B_s^-$  distribution, while the red dashed line shows the corresponding background component. (Right) Opposite-sign  $Q$  distribution (closed circles) in the  $0 < Q < 50$  MeV range, along with the result of the signal-plus-background fit (blue solid curve); the background term is also shown (red dashed curve).

## 2. Measurement of the $B_s$ lifetime difference

The decay of a  $B_s$  meson is characterized by the possibility that it may go through the mixing between its two flavor eigenstates ( $B_s - \bar{B}_s$ ). The resulting mass eigenstates from mixing are expected to have sizable mass and decay width difference. Since the CP-violating mixing phase is expected to be small in the Standard Model, the two mass eigenstates are approximately equal to CP eigenstates. The light mass eigenstate is expected to be a CP-even state with a shorter lifetime than the heavy mass eigenstate which is a CP-odd state. The decay width difference of the two  $B_s$  eigenstates is found to be several percent of the mean decay rate. In the decay  $B_s \rightarrow J/\psi\phi$  with  $J/\psi \rightarrow \mu^+\mu^-$  and  $\phi \rightarrow K^+K^-$ , the final state is an admixture of the CP-even and CP-odd eigenstates. A measurement of the lifetime difference ( $\Delta\Gamma_s$ ) of the two mass eigenstates can be performed using the proper decay time distribution of  $B_s$  meson. The additional information required to separate the light and heavy mass eigenstates can be obtained from the angular distribution of the final decay products.

The  $J/\psi$  candidates are reconstructed from two oppositely charged muon pairs that originated from a common vertex with an invariant mass lies within 150 MeV of the world-average  $J/\psi$  mass [1]. Candidate  $\phi(1020)$  mesons are reconstructed from pairs of oppositely charged tracks with  $p_T > 0.7$  GeV, that are selected from a sample where all the muon candidate tracks forming the  $J/\psi$  candidate have been removed. Each such track is assumed to be a kaon and the invariant mass of a track pair is required to be within 10 MeV of the world average  $\phi(1020)$ -meson mass [1].

The  $B_s$  candidates are formed by combining a  $J/\psi$  with a  $\phi(1020)$  candidate. The two muons and the two kaons are subjected to a combined vertex and kinematic fit, where the dimuon invariant mass is constrained to the nominal  $J/\psi$  mass [1]. The  $B_s$  candidates are selected if the

corresponding  $(J/\psi, \phi)$  pair has an invariant mass between 5.20 and 5.65 GeV, and a  $\chi^2$  vertex-fit probability larger than 2%. For events with more than one  $B_s$  candidate, that with the highest vertex-fit probability is selected.

An un-binned maximum likelihood fit to the data is performed by including the information on the invariant mass, proper decay time and the three decay angles of the reconstructed  $B_s$  candidates. The fit is applied to the sample of 19,200 candidates, selected in the mass range [5.24 - 5.49] GeV and proper decay length range [0.02 - 0.3] cm. From this five-dimensional fit, the physics parameters of interest  $\Delta\Gamma_s$ ,  $\Gamma_s$ ,  $|A_{\perp}^2|$ ,  $|A_{\parallel}^2|$  and  $\delta_{\parallel}$  are determined, assuming that the mixing phase  $\phi_s$  is zero.

The mass distribution of the reconstructed  $B_s$  candidates is shown in Fig. 2(left), together with the overlaid five-dimensional fit projection. The measured signal yield is  $14456 \pm 140$ , with a fitted mass mean of  $5366.8 \pm 0.1$  MeV. The full fit was finally performed in the full mass range, and the one-dimensional projections on the distributions of the proper decay length distributions and the angular variables are shown in Fig. 2(right) and Fig. 3 respectively.

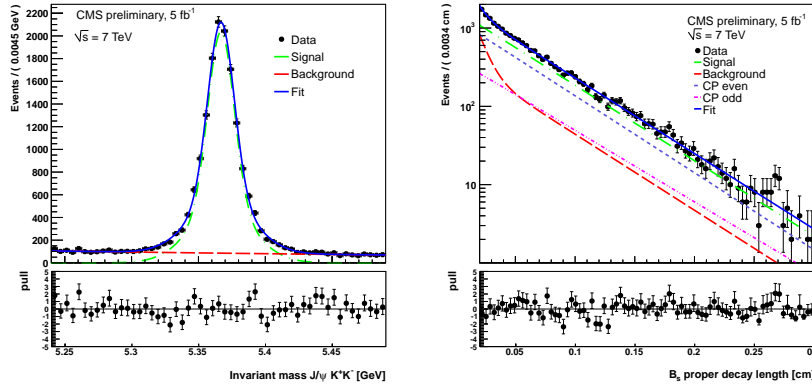


**Figure 2:** (Left) Mass projection of the five-dimensional maximum likelihood fit to the data. The points are the data distribution, the solid blue line shows the full fit, the green dash-dotted line is the signal model component, the red long-dashed line is the background component. The pull between the mass distribution and the fit is shown in the histogram below. (Right) Proper decay length projection of the five-dimensional maximum likelihood fit to the data. The points are the data distribution, the solid blue line shows the full fit, the green dash-dotted line is the signal model component, with the CP-even (odd) component shown in blue short dashed line (magenta dash-dot-dotted line), and the red long dashed line is the background component. The pull between the proper decay length distribution and the fit is shown in the histogram below.

The  $B_s$  decay width difference,  $B_s$  mean lifetime, transversity amplitudes ( $|A_{\perp}^2|$  and  $|A_{\parallel}^2|$ ) and the strong phase  $\delta_{\parallel}$  are measured to be

$$\begin{aligned}\Delta\Gamma_s &= 0.048 \pm 0.024(stat.) \pm 0.003(syst.) ps^{-1}, \\ t_{B_s} &= 0.04580 \pm 0.00059(stat.) \pm 0.00022(syst.) cm, \\ |A_{\perp}^2| &= 0.528 \pm 0.010(stat.) \pm 0.015(syst.), \\ |A_{\parallel}^2| &= 0.251 \pm 0.013(stat.) \pm 0.014(syst.), \\ \delta_{\parallel} &= 2.79 \pm 0.14(stat.) \pm 0.19(syst.) rad.\end{aligned}$$

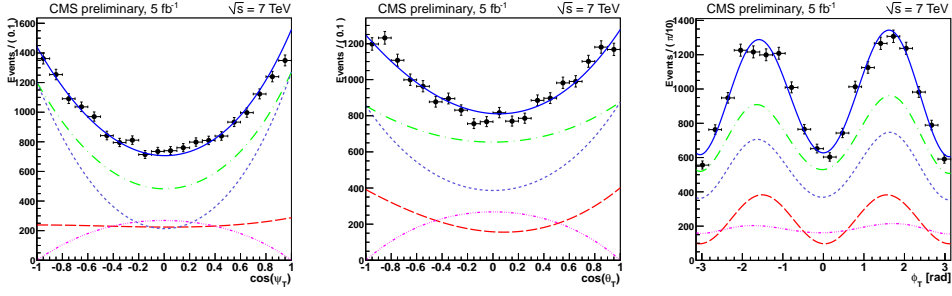


**Figure 3:** The angular projection of the five-dimensional maximum likelihood fit to the data. The plots show the projections on the angular variables  $\cos(\psi_T)$ ,  $\cos(\theta_T)$  and the angle  $\phi$

### 3. Measurement of the $\Lambda_b$ cross section and the $\bar{\Lambda}_b$ to $\Lambda_b$ ratio

Measurements of b-hadron production at 7 TeV represent a test of theoretical approaches that aim to describe heavy-flavor production at the new center-of-mass energy. Furthermore, understanding the production rates for b hadrons represents an essential component in accurately estimating heavy-quark backgrounds for various searches, such as  $H^0 \rightarrow b\bar{b}$  and supersymmetric or exotic new physics signatures with b quarks.

This study presents the first measurement of the production cross section of a b baryon,  $\Lambda_b$ , from fully reconstructed  $J/\psi\Lambda$  decays in pp collisions at  $\sqrt{s} = 7$  TeV and complements the measurements of  $B^+$  [2],  $B^0$  [3], and  $B_s^0$  [4] production cross sections also performed by CMS experiment.

Events with  $\Lambda_b$  baryons reconstructed from their decays to the final state  $J/\psi\Lambda$ , with  $J/\psi \rightarrow \mu^+\mu^-$  and  $\Lambda \rightarrow p\pi$ , are used to measure the differential cross sections  $d\sigma/dp_T^{\Lambda_b} \times B(\Lambda_b \rightarrow J/\psi\Lambda)$ ,  $d\sigma/dy^{\Lambda_b} \times B(\Lambda_b \rightarrow J/\psi\Lambda)$ , and  $\sigma(\bar{\Lambda}_b)/\sigma(\Lambda_b)$  with respect to the transverse momentum  $p_T^{\Lambda_b}$  and the rapidity  $|y^{\Lambda_b}|$ , as well as the integrated cross section times branching fraction for  $p_T^{\Lambda_b} > 10$  GeV and  $|y^{\Lambda_b}| < 2.0$ .

Opposite-sign muon pairs are fit to a common vertex to form  $J/\psi$  candidates, which are required to be within 150MeV of the world-average  $J/\psi$  mass [1]. The  $\Lambda$  candidates are formed by fitting oppositely charged tracks to a common vertex. The invariant mass  $m_{p\pi}$  is required to be within 8MeV of the world-average  $\Lambda$  mass [1]. Candidates are rejected if  $m_{\pi^+\pi^-}$  is within 20MeV of the world-average  $K_S^0$  mass [1].

The  $\Lambda_b$  candidates are formed by combining a  $J/\psi$  candidate with a  $\Lambda$  candidate. A vertex constrained fit is performed with the two muons and the  $\Lambda$  candidate, with the invariant masses of the  $J/\psi$  and  $\Lambda$  candidates constrained to their world-average values [1]. The  $\Lambda_b$  vertex fit confidence level is required to be greater than 1% and the reconstructed  $\Lambda_b$  mass must satisfy  $5.2 < m_{J/\psi\Lambda} < 6.0$  GeV.

The  $\Lambda_b$  yields are extracted from un-binned extended maximum-likelihood fits to the  $m_{J/\psi\Lambda}$  distribution in bins of  $p_T^{\Lambda_b}$  and  $|y^{\Lambda_b}|$ . In each bin, the signal is described by a double-Gaussian function with resolution parameters fixed to values found when fitting simulated signal events and means set to a common value left free in the fit. The background shape is modeled with a third-order polynomial, whose parameters are left free to float independently in each bin. The ratio of

antiparticle to particle yields is obtained by simultaneously fitting the  $\Lambda_b$  and  $\bar{\Lambda}_b$  mass distributions, with resolution parameters fixed from the fit to the combined  $\Lambda_b$  and  $\bar{\Lambda}_b$  simulated sample and common mean allowed to float. The background shapes are fit with separate third-order polynomials, whose parameters are left free in the fit.

Fig. 4 shows the fits to the  $m_{J/\psi\Lambda}$  distributions for  $\Lambda_b$  and  $\bar{\Lambda}_b$  candidates in the inclusive sample with  $p_T^{\Lambda_b} > 10$  GeV and  $|y^{\Lambda_b}| < 2.0$ . The total number of signal events extracted from an inclusive fit is  $1252 \pm 42$ , where the uncertainty is statistical only.

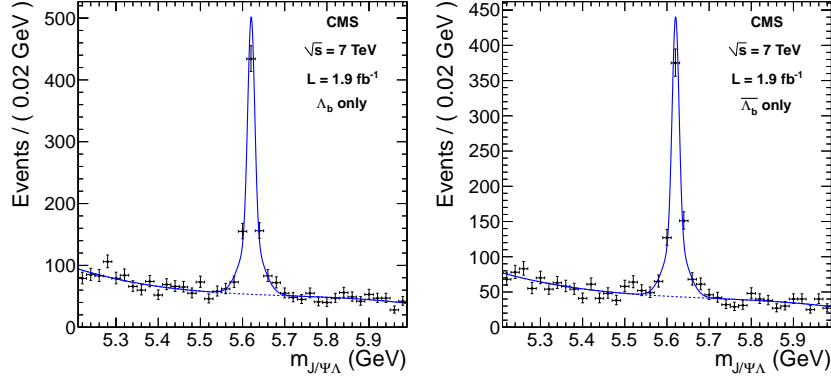


**Figure 4:** Fit results for the  $m_{J/\psi\Lambda}$  distributions for  $\Lambda_b$  and  $\bar{\Lambda}_b$  candidates in the inclusive sample with  $p_T^{\Lambda_b} > 10$  GeV and  $|y^{\Lambda_b}| < 2.0$ , where the dashed line shows the background fit function, the solid line shows the sum of signal and background, and the points indicate the data.

A comparison of the measured  $\Lambda_b$  differential cross section and previous CMS results for b-hadron production versus  $p_T$  is shown in Fig. 5, where the data are fit to the Tsallis function [5]

$$\frac{1}{N} \frac{dN}{dp_T} = C p_T \left[ 1 + \frac{\sqrt{p_T^2 + m^2} - m}{nT} \right]^{-n}. \quad (3.1)$$

Here C is a normalization parameter, T and n are shape parameters, m is the mass of the b hadron and N is the b-hadron yield. The statistical and bin-to-bin systematic uncertainties are used in the fits. The T parameter represents the inverse slope parameter of an exponential, which dominates at low  $p_T$ . Since our data do not constrain that region well, T is fixed to the mean value found from fitting the  $B^+$  and  $B^0$  distributions, where the  $p_T$  threshold is lowest. The result of  $T = 1.10$  GeV is used to obtain the following values of the n parameter, which controls the power-law behavior at high  $p_T$ :  $n(B^+) = 5.5 \pm 0.3$ ,  $n(B^0) = 5.8 \pm 0.3$ ,  $n(B_s^0) = 6.6 \pm 0.4$ , and  $n(\Lambda_b) = 7.6 \pm 0.4$ . The larger n value for  $\Lambda_b$  indicates a more steeply falling  $p_T$  distribution than observed for the mesons, also suggesting that the production of  $\Lambda_b$  baryons, relative to B mesons, varies as a function of  $p_T$ , with a larger  $\Lambda_b/B$  ratio at lower transverse momentum.

The ratio  $\sigma(\bar{\Lambda}_b)/\sigma(\Lambda_b)$  versus  $p_T^{\Lambda_b}$  and  $|y^{\Lambda_b}|$  are shown in Fig. 6. The ratio  $\sigma(\bar{\Lambda}_b)/\sigma(\Lambda_b)$  is found to be consistent with unity and constant as a function of both  $p_T^{\Lambda_b}$  and  $|y^{\Lambda_b}|$  within the uncertainties, as predicted by POWHEG and PYTHIA.

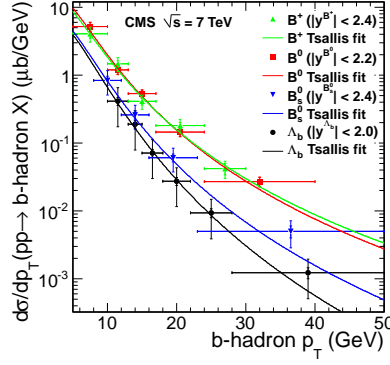


**Figure 5:** Comparison of production rates for  $B^+$ ,  $B^0$ ,  $B_s^0$ , and  $\Lambda_b$  versus  $p_T$ . The plot shows the absolute comparison, where the inner error bars correspond to the total bin-to-bin uncertainties, while the outer error bars represent the total bin-to-bin and normalization uncertainties added in quadrature. Fits to the Tsallis function for each distribution are also shown. The overall uncertainties for  $B_s^0$  and  $\Lambda_b$  are dominated by large uncertainties on  $B(B_s^0 \rightarrow J/\psi\phi)$  and  $B(\Lambda_b \rightarrow J/\psi\Lambda)$ , respectively.

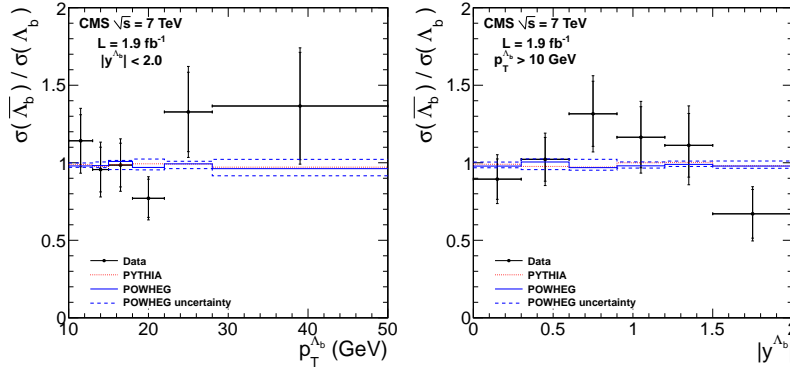


**Figure 6:** Measured  $\sigma(\bar{\Lambda}_b)/\sigma(\Lambda_b)$  (points) versus  $p_T^{\Lambda_b}$  (left) and  $|y^{\Lambda_b}|$  (right), compared to the theoretical predictions from PYTHIA (red dashed line) and POWHEG (blue solid line). The inner error bars correspond to the statistical uncertainties, and the outer error bars represent the uncorrelated systematic uncertainties added in quadrature to the statistical uncertainties. The dashed blue lines show the uncertainties of the POWHEG predictions.

## References

- [1] K. Nakamura *et al.*, "Review of particle physics", J.Phys.G G37 (2010) 075021.
- [2] CMS Collaboration, "Measurement of the  $B^+$  Production Cross Section in pp Collisions at  $\sqrt{s} = 7$  TeV" Phys. Rev. Lett. **106**, (2011) 112001
- [3] CMS Collaboration, "Measurement of the  $B^0$  Production Cross Section in pp Collisions at  $\sqrt{s} = 7$  TeV" Phys. Rev. Lett. **106**, (2011) 252001
- [4] CMS Collaboration, "Measurement of the  $B_s^0$  Production Cross Section with  $B_s^0 \rightarrow J/\psi\phi$  Decays in pp Collisions at  $\sqrt{s} = 7$  TeV" Phys. Rev. D **84**, (2011) 052008
- [5] C. Tsallis, "Possible Generalization of Boltzmann-Gibbs Statistics", J. Stat. Phys. **52**, (1988) 479